# Diffusion-weighted magnetic resonance imaging in the characterization of odontogenic cysts and tumors

Rajesh Vanagundi, MD,[a] Jyoti Kumar, MD,[a] Alpana Manchanda, MD,[a] Sujata Mohanty, MS,[b] and Ravi Meher, MS[c]

**Objectives.** The aim of this study was to evaluate diffusion-weighted imaging (DWI) in comparison with morphologic magnetic resonance imaging (MRI) in differentiating among odontogenic keratocyst (OKC), unicystic ameloblastoma (UAB), and dentigerous cyst (DC).

**Study Design.** Contrast-enhanced MRI, including DWI, was performed on 27 patients with the 3 lesions. Signal intensity characteristics were evaluated on T1- and T2-weighted MRI. The apparent diffusion coefficient (ADC) cutoff value to most effectively differentiate among the 3 lesions was calculated with receiver operating characteristic analysis.

**Results.** In total, 17 OKCs, 5 UABs, and 5 DCs were diagnosed histologically. There were no significant differences among them in signal intensity on T1- or T2-weighted images ($P \geq .13$). On DWI, 14 of 17 OKCs showed restricted diffusion with a mean ADC value of $0.954 \times 10^{-3}$ mm$^2$/s. All 5 UABs and all 5 DCs exhibited facilitated diffusion with ADC values $\geq 2.150 \times 10^{-3}$ mm$^2$/s. The ADC cutoff to differentiate OKCs from UABs was $2.137 \times 10^{-3}$ mm$^2$/s ($P = .01$); UABs from DCs was $2.422 \times 10^{-3}$ mm$^2$/s ($P = .03$); and OKCs from DCs was $2.347 \times 10^{-3}$ mm$^2$/s ($P = .01$).

**Conclusions.** Addition of diffusion-weighted sequences to MRI jaw protocols can assist in the characterization of OKCs, UABs, and DCs. (Oral Surg Oral Med Oral Pathol Oral Radiol 2020;130:447−454)

Conventional radiographic techniques, such as intraoral and panoramic radiography, form the traditional foundation for the evaluation of jaw lesions. The arch-like configuration of the jaws and the superimposition of teeth hamper the diagnostic accuracy of these conventional techniques.[1] These radiographs are also of limited value in the assessment of lesion size, margins, and extension. These limitations have been overcome, to a large extent, by the advent of cross-sectional imaging techniques, including multidetector computed tomography (MDCT) and magnetic resonance imaging (MRI). However, there is considerable overlap among the morphologic characteristics of various odontogenic jaw lesions even on MDCT and conventional MRI.

Odontogenic jaw lesions include radicular cyst, odontogenic keratocyst (OKC), unicystic ameloblastoma (UAB), dentigerous cyst (DC), odontogenic myxoma, adenomatoid odontogenic tumor, and calcifying epithelial odontogenic tumor. Among the above-mentioned odontogenic lesions, OKC, UAB, and DC constitute the majority of noninflammatory jaw lesions encountered in clinical practice and require cross-sectional imaging modalities for their diagnosis and management.

Treatment planning of OKC is variable, ranging from a conservative approach to radical surgery, depending on the lesion's size and aggressive nature.[2] Management of patients with ameloblastoma is almost always with resection.[3] However, UAB has a more favorable prognosis and generally responds to conservative management approaches, including enucleation with curettage or marsupialization.[4] DC is usually treated with enucleation or marsupialization, depending on whether or not the impacted tooth needs to be preserved. Because there are different treatment strategies for different types of jaw lesions, radiologic diagnosis of these lesions plays a significant role in surgical planning.

Ameloblastomas demonstrate both enhancing solid components and nonenhancing cystic components on cross-sectional imaging.[5] The enhancing solid component of ameloblastomas can be used to differentiate them from peripherally enhancing OKCs or DCs on contrast-enhanced MDCT and MRI.[6] However, UABs can be extremely difficult to differentiate from OKCs and DCs, even with cross-sectional imaging modalities, because of their cyst-like structure.

MRI is most commonly used to evaluate the morphologic features of soft tissues through their depiction

## Statement of Clinical Relevance

Odontogenic keratocyst, unicystic ameloblastoma, and dentigerous cyst have overlapping features on conventional magnetic resonance imaging (MRI) but different treatment protocols. Although these lesions have similar features on MRI, diffusion-weighted imaging can distinguish them from each other.

[a]Department of Radiodiagnosis, Maulana Azad Medical College, New Delhi, India.
[b]Department of Oromaxillofacial Surgery, Maulana Azad Institute of Dental Sciences, New Delhi, India.
[c]Department of Otorhinolaryngology, Maulana Azad Medical College, New Delhi, India.
Received for publication Sep 21, 2019; returned for revision Apr 12, 2020; accepted for publication Apr 14, 2020.

2212-4403/$-see front matter
https://doi.org/10.1016/j.oooo.2020.04.010

in images that are weighted to visualize the individual characteristics of tissues. For example, the intensity of signals in T1- and T2-weighted images (T1WI, T2WI) is often examined in the diagnosis of soft tissue lesions. However, diffusion-weighted imaging (DWI) is a functional MRI technique that has a promising role in differentiating these entities on the basis of the Brownian motion of water molecules in tissues.[7] Lesions with high cellularity restrict this motion and hence impede diffusion, and lesions with lower cellularity exhibit more diffusion. Initially used for the diagnosis of stroke and intracranial neoplasms, DWI is being increasingly used for various head and neck lesions, with only a small increase in imaging time.[8] The amount of water molecule motion in DWI is quantified by the apparent diffusion coefficient (ADC).

The objective of this investigation was to compare the ADC values derived from DWI with the T1WI and T2WI signal intensities obtained from MRI in differentiating among OKCs, UABs, and DCs, with histopathological diagnosis as the gold standard. The null hypotheses stated that there were no statistically significant differences in T1- or T2WI signal intensity or in ADC values among the 3 lesions.

## MATERIALS AND METHODS

The study was conducted prospectively from October 2017 to March 2019. In total, 34 patients with jaw lesions detected on panoramic radiographs were included in the study. The study was approved by the institutional ethics committee (IRBF. No. 11/IEC/MAMC/2016/Radio-D11). Informed consent was obtained from all patients included in the study. All patients received contrast-enhanced MRI, including DWI. The images were analyzed by 2 independent observers with postgraduate degrees in radiodiagnosis, one with 20 years of experience and the other with 15 years of experience in the field of radiology. Consensus on signal intensity was reached among the observers for each case. Each observer calculated ADC values independently.

Multiplanar MRI was conducted on a Magnetom Skyra 3 T MRI scanner (Siemens, Erlangen, Germany) using a neurovascular coil. The following parameters were used to acquire T1WI and T2WI in multiple planes.

- *T1WI:* TR: 700 ms; TE: 9.4 ms; section thickness: 5 mm; voxel size: 0.8 × 0.8 × 3 mm; field of view (FOV) read: 240 mm; FOV phase: 100%
- *T2-weighted turbo spin echo (T2W TSE):* TR: 3000 ms; TE: 78 ms; section thickness: 3 mm; voxel size: 0.5 × 0.5 × 3 mm; FOV read: 200 mm; FOV phase: 100%
- *Short tau inversion recovery (STIR):* TR: 5000 ms; TE: 37 ms; section thickness: 3 mm; voxel size: 0.7 × 0.8 × 3 mm; FOV read: 240 mm; FOV phase: 100%
- *DWI after acquisition of conventional neck MRI:* DWI was obtained in the axial plane by using a single shot echo-planar diffusion weighted sequence without breath hold. Three b-values were used: 50, 400, and 800 s/mm$^2$. Other parameters included TR: 3490 ms; TE: 63 ms; section thickness: 5 mm; total slices: 20; voxel size: 2.3 × 2.3 × 5 mm; phase encoding direction: posterior to anterior; bandwidth: 1860 Hz/Px; echo spacing: 0.64 ms; FOV read: 300 mm; FOV phase: 68.8%
- *Postcontrast T1-weighted fat suppressed (T1W FS):* TR: 585 ms; TE: 10 ms; section thickness: 3 mm; voxel size: 0.5 × 0.5 × 3 mm

Of 34 patients, 30 patients had odontogenic lesions, and the remaining 4 patients had non-odontogenic lesions, as determined on the final histopathological examination. The odontogenic lesions included 17 OKCs, 5 UABs, 3 ameloblastomas, and 5 DCs. The 4 nonodontogenic lesions included 1 case each of fibrous dysplasia, intraosseous hemangioma, multiple myeloma, and osteosarcoma.

Most ameloblastomas contain both enhancing solid cystic components and nonenhancing cystic components on cross-sectional imaging. The enhancing solid components can be used to differentiate these lesions from peripherally enhancing OKCs and DCs. However, UABs can be extremely difficult to distinguish from OKCs and DCs, even with cross-sectional imaging, because of their cyst-like anatomy. Therefore, the 3 ameloblastomas were excluded. The final study sample included 17 OKCs, 5 UABs, and 5 DCs because these lesions may be difficult to differentiate on morphologic imaging alone.

### T1WI and T2WI signal characteristic analysis

The lesions were classified as hypointense, isointense, or hyperintense based on their signal intensity relative to muscle. All lesions included in the study were cystic jaw lesions with peripheral enhancement and no solid component greater than 1 cm$^2$ in size.

Enhancement was further classified into a thin (≤ 3 mm) or thick (> 3 mm) peripheral rim.

### DWI analysis

Each odontogenic lesion was qualitatively and quantitatively analyzed separately. Both DWI and corresponding ADC maps were evaluated. Qualitatively, lesions with a hyperintense signal on b = 800 s/mm$^2$ and a hypointense signal on corresponding ADC maps were characterized as having restricted diffusion. Lesions with loss of signal on b = 800 s/mm$^2$ and a hyperintense signal on ADC maps were considered as having facilitated diffusion. A circular region of interest of at least 1 cm$^2$ was placed within the lesion to calculate ADC values for quantitative analysis. A minimum of 3 ADC values were generated for each component of the lesion, and the mean ADC value was

calculated by each observer independently. The final mean ADC value was then derived by averaging the 2 mean ADC values obtained by each observer. The ADC value was expressed in $mm^2/s \pm$ standard deviation (SD).

### Gold standard

Histopathological diagnosis was performed for all lesions and was considered the gold standard diagnosis.

### Statistical analysis

The ability of the signal intensity of MRI to distinguish among OKCs, UABs, and DCs was analyzed with the $\chi^2$ test for T1WI and T2WI. To assess the accuracy of the ADC values for differentiation of these lesions, receiver operating characteristic (ROC) analysis was performed. After the ROC curves were obtained, the Youden method was applied to determine the optimal ADC cutoff value to differentiate among OKCs, UABs, and DCs. A *P* value less than .05 was considered statistically significant. Statistical analysis was done with the SPSS software version 17 (SPSS Inc., Chicago, IL).

## RESULTS

Of the 27 lesions, 17 were diagnosed as OKCs, 5 as UABs, and 5 as DCs on histopathological examination and on MRI.

Of the 17 lesions diagnosed as OKCs, conventional MRI T1WI sequences showed a hypointense signal in 9 cases (52.9%) and a hyperintense signal in 8 cases (47.1%). On T2WI, a hypointense to isointense signal was seen in 4 cases (23.5%) and a hyperintense signal in 13 cases (76.5%). Postcontrast scans revealed all OKCs to have a peripheral rim of enhancement, in which a thin rim was observed in 11 lesions (64.7%) and a thick rim in 6 lesions (35.3%). DWI analysis revealed that 14 of the 17 lesions (82.4%) had restricted diffusion, with a mean ADC value of $0.954 \times 10^{-3}$ $mm^2/s$, and 3 (17.6%)

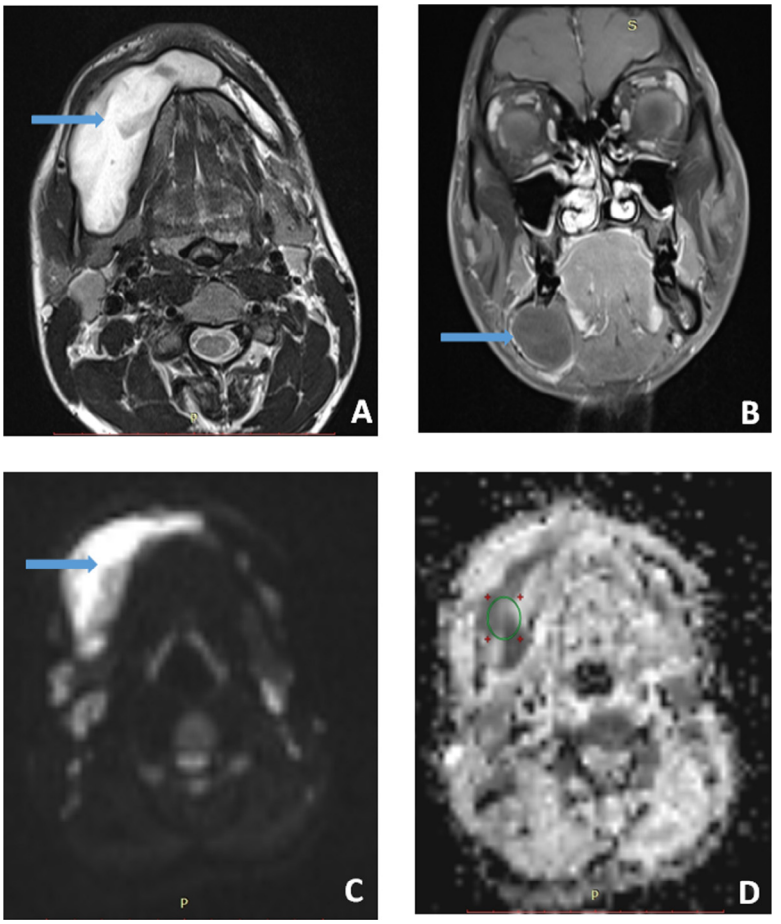


Fig. 1. **A–D,** An 18-year-old male patient with odontogenic keratocyst (OKC). Axial T2-weighted image **(A)** shows a well-defined hyperintense lesion *(blue arrow)* involving the body of the right mandible extending to the midline. Postcontrast coronal T1-weighted image **(B)** shows thin peripheral rim enhancement of the lesion. Axial diffusion-weighted imaging (DWI) scan at b-value = 800 $s/mm^2$ **(C)** reveals high signal intensity of the lesion *(blue arrow)* with a corresponding apparent diffusion coefficient (ADC) map **(D)** showing loss of signal suggestive of restricted diffusion *(green circle)*. Mean ADC value of the lesion is $0.827 \times 10^{-3}$ $mm^2/s$.

exhibited facilitated diffusion with a mean ADC value of 2.217 × $10^{-3}$ $mm^2/s$. The mean ADC value for all 17 lesions was 1.582 × $10^{-3}$ $mm^2/s$. A representative lesion is depicted in Figure 1.

All 5 cases of UAB had a hypointense T1WI signal and a hyperintense T2WI signal. The lesion was classified as unicystic if it exhibited only rim enhancement or when the solid enhancing portion was less than 1 $cm^2$. On DWI, all 5 lesions were characterized by facilitated diffusion, with a mean ADC value of 2.518 × $10^{-3}$ $mm^2/s$. A representative case of UAB is shown in Figure 2.

On conventional MRI, 2 of the 5 DCs (40%) had a hypointense T1WI signal, with 3 of the 5 lesions (60%) exhibiting an isointense to hyperintense signal. All 5 lesions showed a hyperintense signal on T2WI. On contrast-enhanced MRI, all 5 cases exhibited a peripheral thin rim of enhancement. On DWI, all 5 DCs showed facilitated diffusion, with a mean ADC value of 2.150 × $10^{-3}$ $mm^2/s$. A representative lesion is depicted in Figure 3.

The signal intensities of the OKCs, UABs, and DCs are depicted as in Table I. There were no statistically significant differences in either the T1WI ($P$ = .13) or T2WI ($P$ = .26) signal intensity for OKCs, UABs, and DCs.

DWI characteristics of the OKCs, UABs, and DCs are listed in Table II. Both qualitative and quantitative results were analyzed.

On qualitative analysis, 14 of the 17 cases of OKC showed restricted diffusion, whereas all cases of UAB and DC exhibited facilitated diffusion.

For quantitative analysis, the Youden method was applied to the ROC data to determine the optimal ADC cutoff values of OKC, UAB, and DC. An ADC value of 2.137 × $10^{-3}$ $mm^2/s$ produced a statistically significant difference between the ADC values of OKC and those of UAB ($P$ =.01). The area under the ROC curve was 0.94 (95% confidence interval [CI] 0.85−0.99) with sensitivity of 100% and specificity of 85.7% (Figure 4).

An ADC value of 2.422 × $10^{-3}$ $mm^2/s$ resulted in a statistically significant difference between the ADC values

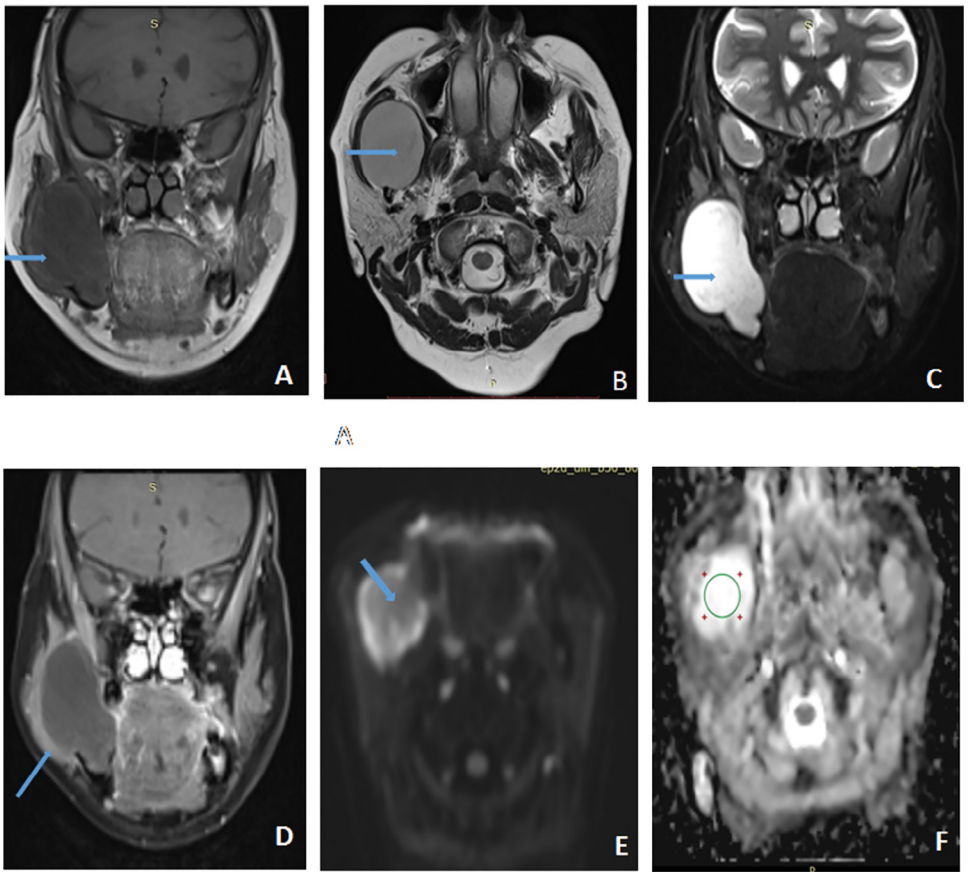


Fig. 2. **A−F,** A 48-year-old female patient with unicystic ameloblastoma (UAB). Coronal T1-weighted image **(A)** shows a well-defined hypointense lesion *(blue arrow)* in the body and ramus of the mandible on the right side. Axial T2 and coronal STIR images **(B, C)** show the lesion *(blue arrow)* with high signal intensity. Coronal T1-weighted image **(D)** shows thin peripheral rim enhancement *(blue arrow)*. Axial diffusion-weighted imaging (DWI) scan **(E)** shows a hypointense signal *(blue arrow)* with hyperintensity on the corresponding apparent diffusion coefficient (ADC) map **(F)** suggestive of facilitated diffusion *(green circle)*. Mean ADC value of the lesion is 2.315 × $10^{-3}$ $mm^2/s$.

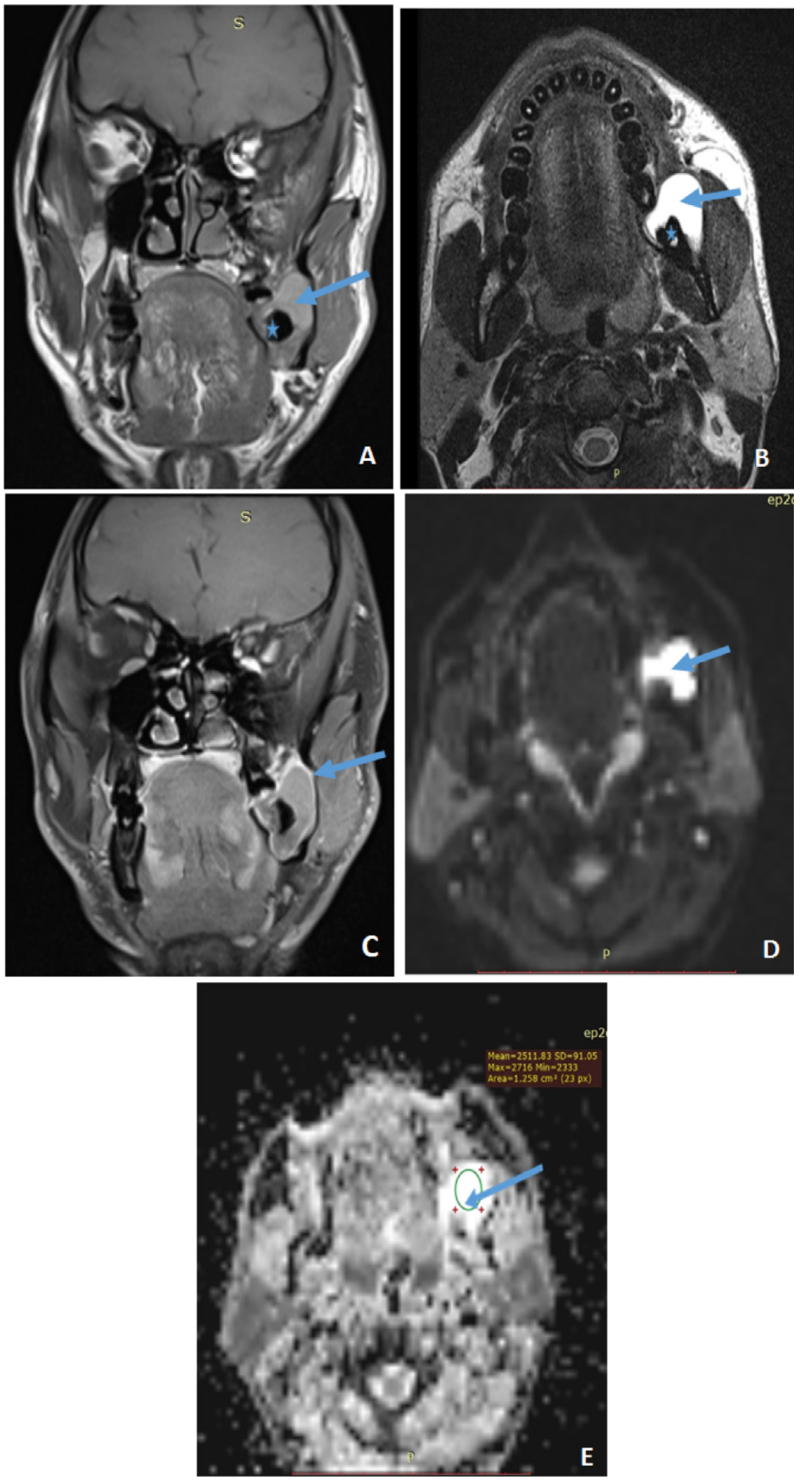


Fig. 3. **A**–**E,** A 28-year-old male patient with dentigerous cyst (DC). Coronal T1-weighted magnetic resonance imaging (MRI) scan **(A)** shows a well-defined lesion *(blue arrow)*, with an associated impacted tooth *(asterisk)* appearing mildly hyperintense relative to muscle. Axial T2-weighted MRI scan **(B)** shows markedly hyperintense signal intensity of the lesion *(blue arrow)* surrounding the impacted tooth *(asterisk)*. Coronal postcontrast T1-weighted MRI scan **(C)** shows a peripheral thin rim (~ 2 mm) of enhancement. Axial diffusion-weighted imaging (DWI) scan at b-800 $mm^{-2}$/sec **(D)** and corresponding apparent diffusion coefficient (ADC) map **(E)**, both reveal a hyperintense signal *(blue arrows in D and E, green circle in E)*, suggestive of facilitated diffusion with a mean ADC value of 2.511 $\times$ $10^{-3}$ $mm^2$/s.

**Table I.** Signal characteristics of odontogenic keratocyst (OKC), unicystic ameloblastoma (UAB), and dentigerous cyst (DC)

| *Lesion* | *T1WI* | | *T2WI* | |
|---|---|---|---|---|
| | *Hypointense* | *Isointense/Hyperintense* * | *Hypointense/Isointense*† | *Hyperintense* |
| OKC (n = 17) | 9 | 8 | 4 | 13 |
| UAB (n = 5) | 5 | 0 | 0 | 5 |
| DC (n = 5) | 2 | 3 | 0 | 5 |

There were no statistically significant differences in the signal intensities of T1WI or T2WI for OKC, UAB, and DC.
*T1WI: P* = .13.
*T2WI: P* = .26.
*On T1WI, 3 of 5 cases of DC showed a isointense to hyperintense signal.
†On T2WI, 4 of 17 cases of OKC showed a hypointense to isointense signal.

**Table II.** Diffusion-weighted imaging characteristics of odontogenic keratocyst (OKC), unicystic ameloblastoma (UAB), and dentigerous cyst (DC)

| *Lesion* | *Qualitative analysis* | | *Quantitative analysis: Mean ADC value* ($\times 10^{-3}$ *mm²/s) (restricted diffusion)* | *Quantitative analysis: Mean ADC value* ($\times 10^{-3}$ *mm²/s) (facilitated diffusion)* |
|---|---|---|---|---|
| | *Restricted diffusion* | *Facilitated diffusion* | | |
| OKC (n = 17) | 14 | 3 | 0.954 | 2.217 |
| UAB (n = 5) | 0 | 5 | – | 2.518 |
| DC (n = 5) | 0 | 5 | – | 2.150 |

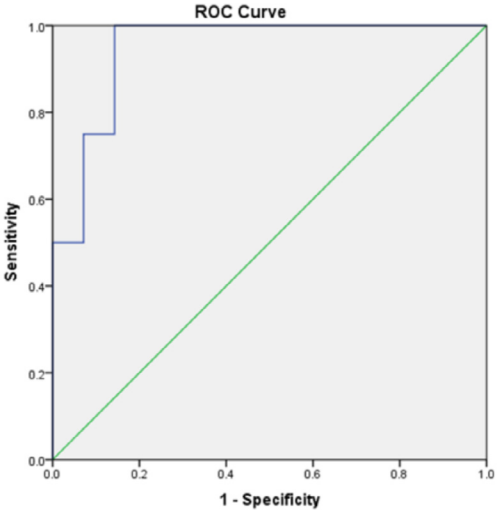


**ROC curve for ADC value between OKC and unicystic ameloblastoma**

Fig. 4. Receiver operating characteristic (ROC) data to determine the optimal apparent diffusion coefficient (ADC) cutoff value between odontogenic keratocyst (OKC) and unicystic ameloblastoma (UAB). The ADC value of 2.137 × $10^{-3}$ $mm^2$/s was statistically significant in differentiating OKC from UAB (*P* = .01), with area under the curve of 0.94 (95% confidence interval [CI] 0.85−0.99), sensitivity of 100%, and specificity of 85.7%.

of UAB and those of DC (*P* =.03). The area under the ROC curve was 0.67 (95% CI 0.34−0.99) with sensitivity of 100% and specificity of 50% (Figure 5).

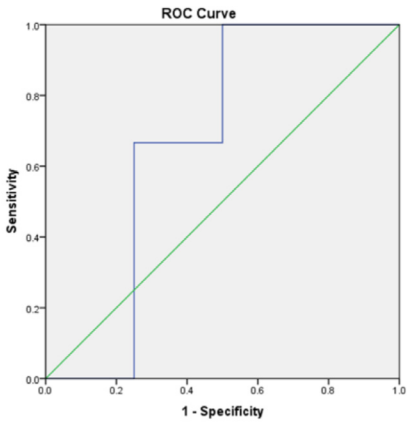


**ROC curve for ADC value between unicystic ameloblastoma and dentigerous cyst**

Fig. 5. Receiver operating characteristic (ROC) data to determine the optimal apparent diffusion coefficient (ADC) cutoff value between unicystic ameloblastoma (UAB) and dentigerous cyst (DC). The Apparent diffusion coefficient (ADC) value of 2.422 × $10^{-3}$ $mm^2$/s was statistically significant in differentiating UAB from DC (*P* = .03), with area under the curve of 0.67 (95% confidence interval [CI] 0.34−0.99), sensitivity of 100%, and specificity of 50%.

An ADC value of 2.347 × $10^{-3}$ $mm^2$ /s produced a statistically significant difference between the ADC values of OKC and those of DC (*P* = .01). The area under the ROC curve was 0.92 (95% CI 0.79−0.99) with sensitivity of 100% and specificity of 92.7% (Figure 6).

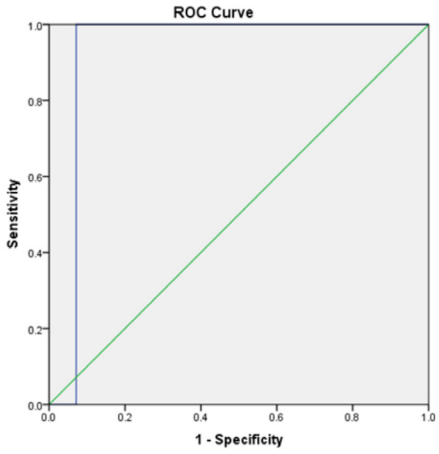


Fig. 6. Receiver operating characteristic (ROC) data to determine the optimal apparent diffusion coefficient (ADC) cutoff value between odontogenic keratocyst (OKC) and dentigerous cyst (DC). The ADC value of 2.347 × $10^{-3}$ $mm^2$/s was statistically significant in differentiating OKC from DC ($P$ = .01), with area under the curve of 0.92 (95% confidence interval [CI] 0.79−0.99), sensitivity of 100%, and specificity of 92.7%.

## DISCUSSION

OKCs, UABs, and DCs are the most common noninflammatory odontogenic lesions in the maxillomandibular region.[9] In a majority of patients, ameloblastoma usually presents as a multilocular lesion with enhancing solid cystic components, nonenhancing cystic components, and peripherally enhancing cystic components. However, some cases may be of the unicystic type, where the lesions are predominantly cystic. These cases are difficult to differentiate from OKC and DC on morphologic evaluation. In these cases, DWI sequences aid in their differentiation.

Of the 17 cases of OKC, 9 lesions (52.9%) exhibited a hypointense signal on T1WI, whereas 8 lesions (47.1%) showed an isointense to hyperintense signal intensity. The hyperintense signal on T1WI is attributed to the keratinaceous contents of the cyst. On T2WI, a hypointense to isointense signal was detected in 4 lesions (23.5%), with a hyperintense signal detected in 13 cases (76.5%).

The imaging features of OKC on MRI were similar to those reported by Konouchi et al.,[10] who discovered that the T1 signal characteristic of OKCs varied from high to intermediate signal intensity. These lesions exhibited a heterogeneous, intermediate-to-high signal intensity on T2WI, with a peripheral thin or thick rim of enhancement on postcontrast imaging.

In our study, 14 of the 17 cases (82.4%) of OKC showed restricted diffusion, with a mean ADC value of 0.954 × 10-3 $mm^2$/s, whereas facilitated diffusion was seen in only 3 lesions (17.6%); these lesions had a mean ADC of 2.217 × 10-3 $mm^2$/s (see Table II). The restricted diffusion seen in OKCs can be explained by the presence of desquamated keratin and hyaluronic acid contents within the cyst lumen. These contents increase the viscosity of the cysts, thereby restricting the diffusion of free water molecules. The facilitated diffusion seen in 3 of 17 cases may be attributed to low keratinaceous content. In a study conducted by Han et al.,[11] all 15 cases of OKC revealed a bright signal on DWI, with a low signal on their corresponding ADC maps, suggesting restricted diffusion.

All 5 cases of UAB revealed a hypointense signal on T1WI and hyperintense signal on T2WI in the present study. These findings were similar to those of the study by Konouchi et al.,[10] who described the signal intensity of UAB as hypointense on T1WI and hyperintense on T2WI. Our findings showed facilitated diffusion, with a mean ADC value of 2.518 × $10^{-3}$ $mm^2$/s (see Table II). These findings were in agreement with the findings from the study by Srinivasan et al.[12] In their study, of the 10 cases of ameloblastoma, 5 were of mixed solid and cystic variety, 3 were predominantly cystic, and the remaining 2 cases were purely cystic. Facilitated diffusion was seen in the cystic components of the lesion, with a mean ADC value of 2.192 × $10^{-3}$ $mm^2$/s.

All of the 5 DCs in our study were unilocular and surrounded an impacted tooth. These findings were similar to those of a study conducted by Zerrin et al.[13] All 9 DCs included in their study were unilocular and associated with impacted third molars. Two of the 5 lesions (40%) in the present investigation exhibited a hypointense signal on T1WI, with the other 3 revealing isointense to hyperintense signals. All 5 cases produced a hyperintense signal on T2WI. On postcontrast imaging, all lesions showed a peripheral thin rim (≤ 3 mm) of enhancement, with no solid component. Pinto et al.[14] reported a case of DC on MRI, in which the lesion produced an intermediate T1 signal and a hyperintense T2 signal. Those authors stated that the hyperintensity on T2WI contributed significantly to the interpretation of a probable cystic lesion rather than a neoplasm.

In our investigation, all cases of DC showed facilitated diffusion, with a mean ADC value of 2.150 × $10^{-3}$ $mm^2$/s (see Table II). This finding is different from the diffusion characteristics of 5 cases of DC in a study by Han et al.[11] Those authors found that DCs had restricted diffusion, with a mean ADC value of 1.257 × $10^{-3}$ $mm^2$/s. They attributed restricted diffusion in DCs to greater viscous content (glycosaminoglycans) within the lesions. A lower concentration of glycosaminoglycans could be the cause of facilitated diffusion in the DCs in our study.

The mean ADC value of all the 17 cases of OKC was 1.582 × $10^{-3}$ $mm^2$/s. This was lower than the mean ADC value obtained for the 5 DCs, which was 2.150 × $10^{-3}$ $mm^2$/s. This is in agreement with the study conducted by Ogura et al.,[15] in which the mean ADC value

of 5 OKCs ($1.03 \pm 0.31 \times 10^{-3}$ mm$^2$/s) was lower than that of 4 DCs ($1.67 \pm 1.06 \times 10^{-3}$ mm$^2$/s).

There was no statistically significant difference in the T1 and T2 signal intensities of OKC, UAB, and DC. The *P* value was .13 for T1 WI and .26 for T2 WI. Because the morphologic features of OKC, UAB, and DC overlap significantly, we tried to evaluate the usefulness of DWI in their differentiation. There was a statistically significant difference ($P = .01$) between the ADC values of OKC and UAB when an ADC value of $2.137 \times 10^{-3}$ mm$^2$/s was used as the optimal cutoff to differentiate them. This cutoff value yielded an area under the ROC curve of 0.94 (95% CI 0.85−0.99), with sensitivity of 100% and specificity of 85.7%. This was similar to the findings in a study conducted by Han et al.,[11] who evaluated the role of DWI in the differentiation of OKC from UAB. They found that the ADC values in the 2 groups were significantly different ($P < .01$). In their study, an ADC value of $2 \times 10^{-3}$ mm$^2$/s was found to be the optimal cutoff, which helped distinguish OKC from UAB, as in our study.

An ADC value of $2.422 \times 10^{-3}$ mm$^2$/s was found to be the optimal cutoff to differentiate UAB from DC, generating an area under the curve of 0.67 (95% CI 0.34−0.99), with sensitivity of 100% and specificity of 50%. There was a statistically significant difference ($P = .03$) between the ADC values of these lesions when this cutoff point was used.

The optimal ADC cutoff value to differentiate between OKC and DC was found to be $2.347 \times 10^{-3}$ mm$^2$/s. This led to an area under the curve value of 0.92 (95% CI 0.79−0.99), with sensitivity of 100% and specificity of 92.7%. The differences in ADC values were significant ($P = .01$).

To the best of our knowledge, the present investigation is the first to analyze the ADC cutoff values to differentiate between UAB and DC and between OKC and DC.

The small number of cases in our study because of low prevalence of these entities was a limitation. Further validation of the results with a larger number of patients is required.

## CONCLUSIONS

Apart from morphologic MRI, which could not produce findings in signal intensity that significantly differed among the 3 types of lesions ($P = .13$ for T1WI and $P = .26$ for T2WI) in our study, functional DWI can be of great benefit in further characterization of these jaw lesions. DWI does not add significantly to cost and duration of the examination but can be of use in differentiating among OKC, UAB, and DC. These lesions have markedly overlapping morphologic features, and preoperative diagnosis has a significant role in planning their management strategy.

## REFERENCES

1. Abrahams JJ. Dental CT imaging: a look at the jaw. *Radiology*. 2001;219:334-345.
2. Dandriyal R, Gupta A, Pant S, Baweja HH. Surgical management of ameloblastoma: conservative or radical approach. *Natl J Maxillofac Surg*. 2011;2:22-27.
3. Hsu M-H, Chaing M-L, Chen J-K. Unicystic ameloblastoma. *J Dent Sci*. 2014;9:407-411.
4. Roopak B, Singh M, Shah A, Patel G. Keratocystic odontogenic tumor: treatment modalities: study of 3 cases. *Niger J Clin Pract*. 2014;17:378-383.
5. Minami M, Kaneda T, Yamamoto H, et al. Ameloblastoma in the maxillomandibular region: MR imaging. *Radiology*. 1992;184:389-393.
6. Fujita M, Matsuzaki H, Yanagi Y, et al. Diagnostic value of MRI for odontogenic tumors. *Dentomaxillofac Radiol*. 2013;42:20120265.
7. Weber AL. History of head and neck radiology: past, present, and future. *Radiology*. 2001;218:15-24.
8. Wang J, Takashima S, Takayama F, et al. Head and neck lesions: characterization with diffusion weighted echo-planar MR imaging. *Radiology*. 2001;220:621-630.
9. Sumi M, Ichikawa Y, Katayama I, Tashiro S, Nakamura T. Diffusion-weighted MR imaging of ameloblastomas and keratocystic odontogenic tumors: differentiation by apparent diffusion coefficients of cystic lesions. *AJNR Am J Neuroradiol*. 2008;29:1897-1901.
10. Konouchi H, Yanagi Y, Hisatomi M, et al. MR imaging diagnostic protocol for unilocular lesions of the jaw. *Jpn Dent Sci Rev*. 2012;48:81-91.
11. Han Y, Fan X, Su L, Wang Z. Diffusion-weighted MR imaging of unicystic odontogenic tumors for differentiation of unicystic ameloblastomas from keratocystic odontogenic tumors. *Korean J Radiol*. 2018;19:79-84.
12. Srinivasan K, Seith Bhalla A, Sharma R, Kumar A, Roy Choudhury A, Bhutia O. Diffusion-weighted imaging in the evaluation of odontogenic cysts and tumours. *Br J Radiol*. 2012;85:e864-e870.
13. Zerrin E, Husniye DK, Peruze C. Dentigerous cysts of the jaws: clinical and radiological findings of 18 cases. *J Oral Maxillofac Radiol*. 2014;2:77-81.
14. Pinto AS, Costa AL, Galvão ND, Ferreira TL, Lopes SL. Value of magnetic resonance imaging for diagnosis of dentigerous cyst. *Case Rep Dent*. 2016;2106:2806235.
15. Ogura I, Nakahara K, Sasaki Y, Sue M, Oda T. Diffusion-weighted magnetic resonance imaging in odontogenic keratocysts: preliminary study on usefulness of apparent diffusion coefficient maps for characterization of normal structures and lesions. *Chin J Dent Res (England)*. 2019;22:51-56.

*Reprint requests:*

Jyoti Kumar
Professor
Department of Radiodiagnosis
Maulana Azad Medical College
Bahadur Shah Zafar Marg
New Delhi 110002
India.
Drjyotikumar@gmail.com